

# The XMM–LSS project: a short presentation of the survey and of the first results

S. Andreon<sup>1</sup>, M. Pierre<sup>2</sup>  
for the XMM–LSS collaboration

<sup>1</sup> INAF–Osservatorio Astronomico di Brera, Italy,  
e-mail: [andreon@brera.mi.astro.it](mailto:andreon@brera.mi.astro.it)

<sup>2</sup> CEA/DSM/DAPNIA, Service d’Astrophysique, Saclay, France

## Abstract.

We (Pierre et al. 2003) have designed a medium deep large area X-ray survey with XMM – the XMM Large Scale Structure survey, XMM-LSS – with the scope of extending the cosmological tests attempted using ROSAT cluster samples to two redshift bins between  $0 < z < 1$  while maintaining the precision of earlier studies. The optimal survey design was found to be an  $8^\circ \times 8^\circ$  area, paved with 10 ks XMM pointing separated by 20 arcmin. This area is the target of several complementary surveys, from the ultraviolet to the radio wavelengths, allowing, beside cosmological studies, detailed studies of the objects included in our area.

**Key words.** X-ray, Large Scale Structures, clusters of galaxies

## 1. Introduction

From a simple theoretical point of view, clusters of galaxies - the most massive bound structures in the Universe - are objects having a mass of the order of  $10^{14-16} M_\odot$  growing by accretion at a rate governed by the initial density fluctuation spectrum, the cosmological parameters, the nature and amount of dark matter as well as the nature of the dark energy. Their 3-dimensional space distribution and number density as functions of cosmic time constrain cosmological parameters in a unique way. Clusters offer considerable advantages for large scale structure (LSS) studies: they

can provide complete samples of objects over a very large volume of space, and they are in crucial respects simple to understand. The extent (and mass) of clusters can be traced by their X-ray emission while the theory describing their formation (biasing) and evolution from the initial fluctuations can be tested with numerical simulations. Such a level of understanding does not exist for galaxies - which have reached a highly non-linear stage - to and even less for QSO and AGN formation. The resulting cluster LSS counts studies can constrain cosmological parameters, independently of Cosmic Microwave Background (CMB) and supernova (SN) studies since they do not rely on the same

---

*Send offprint requests to:* S. Andreon

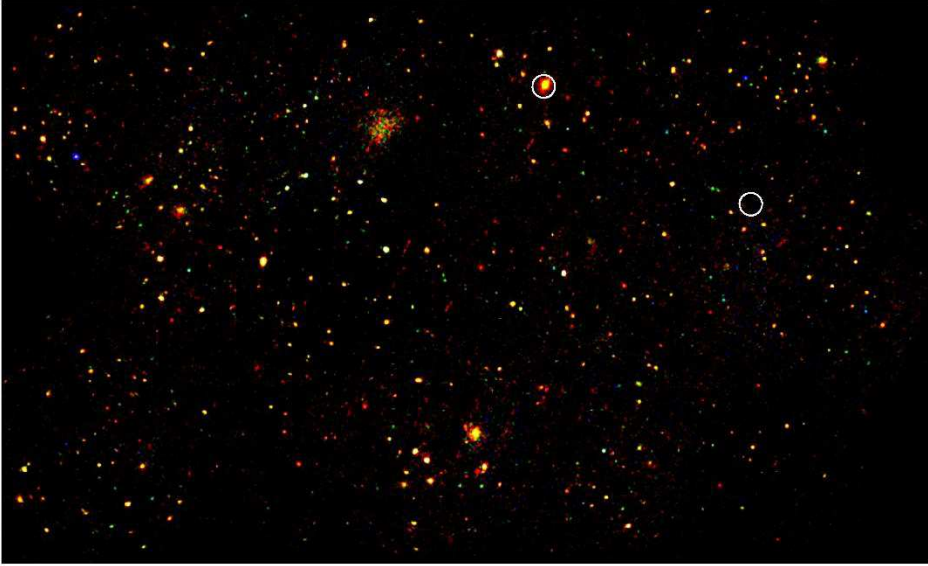


**Fig. 1. First view of the deep X-ray sky on large scales.** Image obtained combining the first 15 XMM-LSS fields mosaiced in true X-ray colours: red [0.3-1.0] keV, green [1.0-2.5] keV, blue [2.5-10.0] keV. The circles indicate the sources found in the RASS; the brightest one being a star, HD14938. The displayed region covers  $1.6 \text{ deg}^2$ . This is the first time that such an X-ray depth has been achieved over such an area. The improvement with respect to the RASS is striking, with a source density of the order of  $\sim 300 \text{ deg}^{-2}$  in the [0.5-2] keV band. The wealth of sources includes supersoft and very hard sources, as well as sources with a wide range of intrinsic extents, giving an indication of the scientific potential of the XMM-LSS survey. The extended source at the top is a cluster of galaxy.

physical processes. A quantitative overview of the cosmological implications of cluster surveys can be found for instance in Haiman, Mohr & Holder (2001).

XMM is in a position to open a new era for X-ray surveys. Its high sensitivity, considerably better PSF than the RASS ( $6''$  on axis) and large field of view ( $30'$ ), make it a

powerful tool for the study of extragalactic LSS. In this respect, two key points may be emphasized. Firstly, a high galactic latitude field observed with XMM at medium sensitivity ( $\sim 0.5 - 1 \cdot 10^{-14} \text{ erg cm}^2 \text{ s}^{-1}$ ) is “clean” as it contains only two types of objects, namely QSOs (pointlike sources) and clusters (extended sources) well above the confusion limit. Secondly, if clusters more luminous than  $L_{[2-10]} \sim 3 \cdot 10^{44} \text{ h}_{70}^{-2} \text{ erg/s}$  are present at high redshift, they can be detected as extended sources out to  $z = 2$ , in XMM exposures of only 10 ks.

## 2. The XMM–LSS survey and the associate surveys

We (Pierre et al. 2003) have designed a survey to yield some 800 clusters in two redshift bins with  $0 < z < 1$ : the XMM Large Scale Structure Survey (XMM-LSS). The optimal survey design was found to be an  $8^\circ \times 8^\circ$  area, paved with 10 ks XMM pointing separated by 20 arcmin (i.e. 9 pointings per degree square). The expected ultimate sensitivity is  $\sim 3 \cdot 10^{-15} \text{ erg cm}^2 \text{ s}^{-1}$  for pointlike sources in the [0.5–2] keV band. It will also trace the LSS as defined by X-ray QSOs out to redshifts of  $\sim 4$ .

In addition, the proposed X-ray survey is associated with several other major new generation surveys (optical, IR, Radio, UV), as detailed in Table 1.

## 3. First results

During fall 2002, we did perform near-infrared observations at NTT of  $z \gtrsim 1$  clusters and trial spectroscopic observations of candidate clusters at VLT and Magellan telescopes. Figure 2 shows an example of a cluster spectroscopically confirmed at  $z = 0.8$  (Valtchanov et al. 2003). Spectroscopic observations confirm 17 out of 18 of the candidate clusters observed (Valtchanov et al. 2003, Willis et al. 2003).

Candidate  $z \gtrsim 1$  clusters are extracted from XMM–LSS database as extended X-ray sources with no obvious optical counterpart (our optical data are deep enough

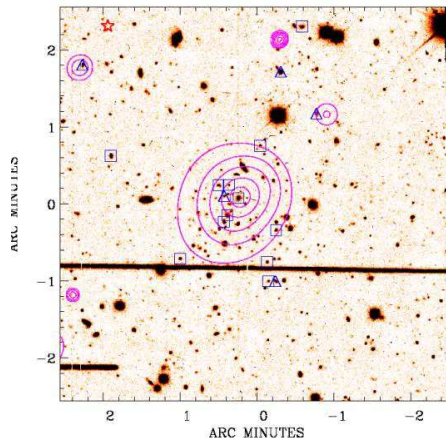


**Fig. 2.** X-ray contours superposed to an I band image of a clusters at  $z = 0.84$ . Marked galaxies are spectroscopic confirmed members. The cluster velocity dispersion, using 17 member galaxies, is  $\sim 800 \text{ km/s}$ . The dark horizontal lines are an artifact due to a nearby bright star.

to detect clusters up to  $z \sim 1$ ) and observed in the near-infrared using SOFI at NTT (Andreon et al. 2003a). The run was very useful, confirming 5  $z \gtrsim 1$  clusters in just over  $1 \text{ deg}^2$  of the survey and suggesting a few  $z \gtrsim 1.3$  clusters. One of the near-infrared confirmed clusters is shown in Figure 3.

The wealth of data available for almost a thousand of clusters allows to study the properties of cluster galaxies, their evolution (both with lookback time and during the infall in the cluster), while keeping the different galaxies classes separated.

Observatory/Instrument	(Planned) Coverage	Band	Final Sensitivity
XMM/EPIC	64 deg <sup>2</sup>	[0.2-10] keV	$\sim 3 \cdot 10^{-15}$ erg cm <sup>2</sup> s <sup>-1</sup> [1]
CFHT/CFH12K (VVDS Deep) *	2 deg <sup>2</sup> GT	B, V, R, I	26.5, 26.0, 26.0, 25.4 [2]
CFHT/CFH12K (VVDS Wide) *	3 deg <sup>2</sup> GO	V, R, I	25.4, 25.4, 24.8 [2]
CFHT/MegaCam	72 deg <sup>2</sup>	u*, g', r', i', z'	25.5, 26.8, 26.0, 25.3, 24.3 [3]
CTIO 4m/Mosaic	$\sim 16$ deg <sup>2</sup>	R, z'	25, 23.5 [4]
UKIRT/WFCAM	8.75 deg <sup>2</sup>	J, H, K	22.5, 22.0, 21.0 [5]
VLA/A-array *	110 deg <sup>2</sup>	74 MHz	275 mJy/beam [6a]
VLA/A-array	5.6 deg <sup>2</sup>	325 MHz	4 mJy/beam [6b]
OCRA	all XMM-LSS clusters	30 GHz	100 $\mu$ Jy [7]
AMiBA	70 deg <sup>2</sup>	95 GHz	3.0 mJy [8]
SIRTF/IRAC (SWIRE Legacy)	8.7 deg <sup>2</sup>	3.6, 4.5, 5.8, 8.0 $\mu$ m	7.3, 9.7, 27.5, 32.5 $\mu$ Jy [9a]
SIRTF/MIPS (SWIRE Legacy)	8.9 deg <sup>2</sup>	24, 70, 160 $\mu$ m	0.45, 6.3, 60 mJy [9b]
Galex	$\sim 20$ deg <sup>2</sup>	1305-3000 Å	$\sim 25.5$ [10]

**Table 1. XMM-LSS X-ray and associated surveys** Notes: \* : complete[1]: for point-like sources in [0.5-2] keV[2]:  $AB_{Mag}$ , 5'' aperture[3]: S/N = 5 in 1.15'' aperture[4]: 4 sigma in 3'' aperture[5]:  $Vega_{Mag}$  [6a]: 30'' resolution; deeper observations planned[6b]: 6.3'' resolution[7]  $5\sigma$ , detection limit[8]  $6\sigma$ , detection limit[9a]  $5\sigma$ [9b]  $5\sigma$ [10]:  $AB_{Mag}$

At the time of this writing, the accumulated sample is already the largest at high redshift ever studied. In a first exploratory study, we focus on the evolution of both the reddest galaxies and of the whole cluster galaxy population. Due to space limitations, we summarize results for only the latter. Figure 4 shows the Schechter (1976) characteristic magnitude,  $m^*$ , in the  $z'$  band ( $\lambda \sim 9000$  Å), for some of our clusters. The upper curve shows the expected relationship between redshift and  $m^*$  if stars do not evolve, and it is clearly rejected by the data. A model in which stars form at  $z_f = 5$  (middle curve) reproduces well the faintest  $m^*$  (at a given redshift, it est the curve traces well the upper envelope of the data points). Clusters with  $m^*$  brighter than the prediction of a  $z_f = 1.3$  model (bottom curve), show a re-youngening, due to a secondary star-formation activity happened at “low” redshift, maybe related to the Butcher–Oemler effect (Butcher & Oemler 1984). The reader is invited to refer to Andreon et al. (2003b) for details.

#### 4. Conclusion

The first optical and spectroscopic observations of the XMM–LSS fields observed dur-

ing the AO-1 period show the feasibility of the cosmological XMM–LSS program, and give interesting results on the galaxy evolution up to  $z = 1$ .

#### References

- Andreon S. et al, 2003a, *in preparation*
- Andreon S. et al, 2003b, *in preparation*
- Butcher, H. & Oemler, A. 1984, ApJ, 285, 426
- Haiman Z., Mohr J. J., Holder G. P., 2001, ApJ, 553, 545
- Pierre et al. 2003, A&A, submitted (astro-ph/0305191)
- Schechter, P. 1976, ApJ, 203, 297
- Valtchanov I. et al 2003, A&A, submitted (astro-ph/0305192)
- Willis et al. 2003, *in preparation*

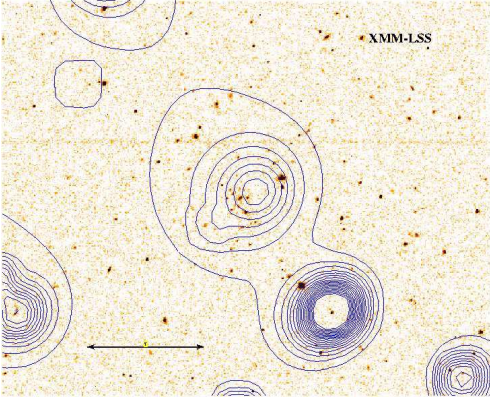


**Fig. 3.** X-ray contours (wavelets filtered) superposed to the  $K$ -band image of one of XMM-LSS clusters at  $z \sim 1.0$ . The photometric redshift of the cluster is derived from the  $R - K$  color of the cluster color-magnitude relation.

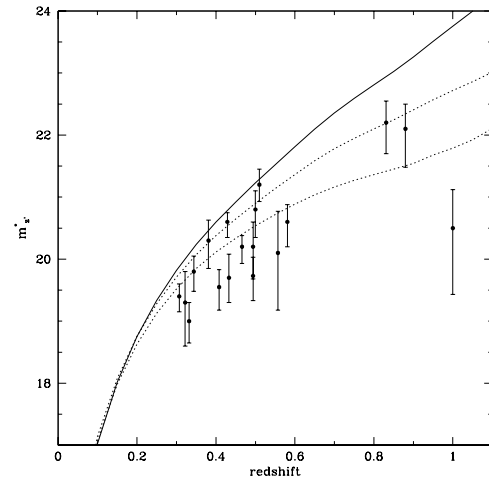


**Fig. 4.** Evolution of  $M^*$  in the  $z'$  filter (points) and model predictions (curves). Three models are plotted in the figure: a model without star aging (top curve), and two models with formation redshifts  $z_f = 5$  (middle curve) and  $z_f = 1.3$  (bottom curve).